AJNR

Spinal cord infection: myelitis and abscess formation.

K J Murphy, J A Brunberg, D J Quint and P H Kazanjian

This information is current as of May 31, 2025.

Spinal Cord Infection: Myelitis and Abscess Formation

Kieran J. Murphy, James A. Brunberg, Douglas J. Quint, and Powel H. Kazanjian

PURPOSE: **Our purpose was to describe the MR findings and evolution of spinal cord abscess and to define those MR features that allow differentiation of cord infection from other intramedullary abnormalities.**

METHODS: **We retrospectively reviewed the MR studies of all patients in whom intramedullary spinal cord abscess was proved either by blood or cerebrospinal fluid culture or by serologic examination at our institution between January 1988 and January 1996. The study group included four adults and two children, 7 to 74 years old (mean age, 38 years).**

RESULTS: **Initial MR studies showed intramedullary high signal on T2-weighted sequences with poorly defined marginal enhancement on T1-weighted images. On follow-up contrast-enhanced T1-weighted studies, the lesions had well-defined enhancing margins with central low signal intensity. After the initiation of therapy, T2 signal abnormalities decreased markedly and contrast-enhanced studies showed ring enhancement. These T1 findings resolved with treatment over serial studies in four patients. The organisms identified were *Streptococcus milleria*, *S pyogenes*, atypical mycobacteria, *Mycobacterium tuberculosis*, and *Schistosoma mansoni* (both children).**

CONCLUSION: **A characteristic sequence of imaging findings aids in the differentiation of cord infection from other intramedullary lesions.**

Intramedullary cord abscesses are uncommon; approximately 70 case have been reported in the literature, with most from the preantibiotic era (1–8). A case was reported in 1830 (2). Courville (3) found only one intramedullary abscess in 40 000 postmortem examinations. Forty percent of abscesses occur in the first two decades of life, with 27% occurring before the age of 10 years (4). Patients with symptoms of less than 4 days' duration have a 90% mortality (5, 6), whereas patients whose symptoms last longer than 7 days have a 67% mortality rate (7). The purpose of this article is to describe the magnetic resonance (MR) imaging findings of spinal cord abscess in six patients, including the evolution of changes seen on follow-up imaging studies in five of them. We define those MR features that allow differentiation of cord infection from other intramedullary abnormalities.

Methods

We identified six patients (five male, one female) with proved intramedullary spinal cord abscess in whom MR studies were obtained at our institution from January 1988 to January 1996. Four patients were adults and two were children (age range, 7 to 74 years; mean age, 38 years). A total of 15 initial and follow-up studies were reviewed. All patients underwent an MR study consisting of a sagittal T1-weighted localizer image, sagittal proton density–weighted studies, T2-weighted fast spin-echo studies, and sagittal and axial T1-weighted spin-echo studies before and after administration of gadopentetate dimeglumine at a dose of 0.1 mmol/kg. Five patients had pretreatment studies. One patient had three follow-up MR studies, three patients had two follow-up studies, two patients had one follow-up study, and one patient had no follow-up studies. The time between the initial study and the first follow-up study ranged from 1 week to 1 month. Five patients had repeated imaging with clinical follow-up for 7 months, 9 months, 3 months, 2 months, and 5 months, respectively. One patient had no repeat imaging after the initial diagnostic studies but had clinical follow-up for 3 months. Clinical follow-up was by discussion with the referring physician. The location, the pattern of enhancement on sagittal and axial T1-weighted sequences, and the pattern of altered signal intensity on T2-weighted images were evaluated. Two patients also had serial brain imaging. All MR examinations were performed at 1.5 T.

No patient had a history of spinal trauma, spinal surgery, malignancy, or adjacent vertebral or epidural disease. One patient was immunocompromised as a result of steroid treat-

FIG 1. Case 1: 28-year-old woman with 10-year history of systemic lupus erythematosus and 10 days of fever, back pain, bilateral lower extremity paresthesia, and weakness. She had been on varying doses of prednisone for the preceding 9 months and was on prednisone (30 mg/day) at the time of presentation. *M tuberculosis* was isolated from cultures of lung tissue and from CSF. Residual gait disturbance was noted at 7-month clinical follow-up.

A–E, MR imaging at the time of presentation. T1-weighted sagittal and axial (T-11 level) images obtained before (*A* and *C*) and after (*B* and *D*) contrast administration show widened anteroposterior and transverse dimensions of the spinal cord with solid intramedullary contrast enhancement (*arrow*). T2-weighted image (*E*) shows central edema extending from the conus to the midthoracic levels (*arrowheads*).

F–H, Persistent cord expansion (*arrows*) is present 5 weeks after initiation of antituberculous treatment on an unenhanced T1-weighted image (*F*) with an area of enhancement (*G*) and increasing cord edema (*H*) on T2-weighted studies.

I–K, Seven months later, the cord is normal in anteroposterior dimension on unenhanced T1-weighted image (*I*), with a smaller persisting region of contrast enhancement (*arrow, J*). A T2-weighted study (*K*) shows only diffuse, mildly increased central signal intensity.
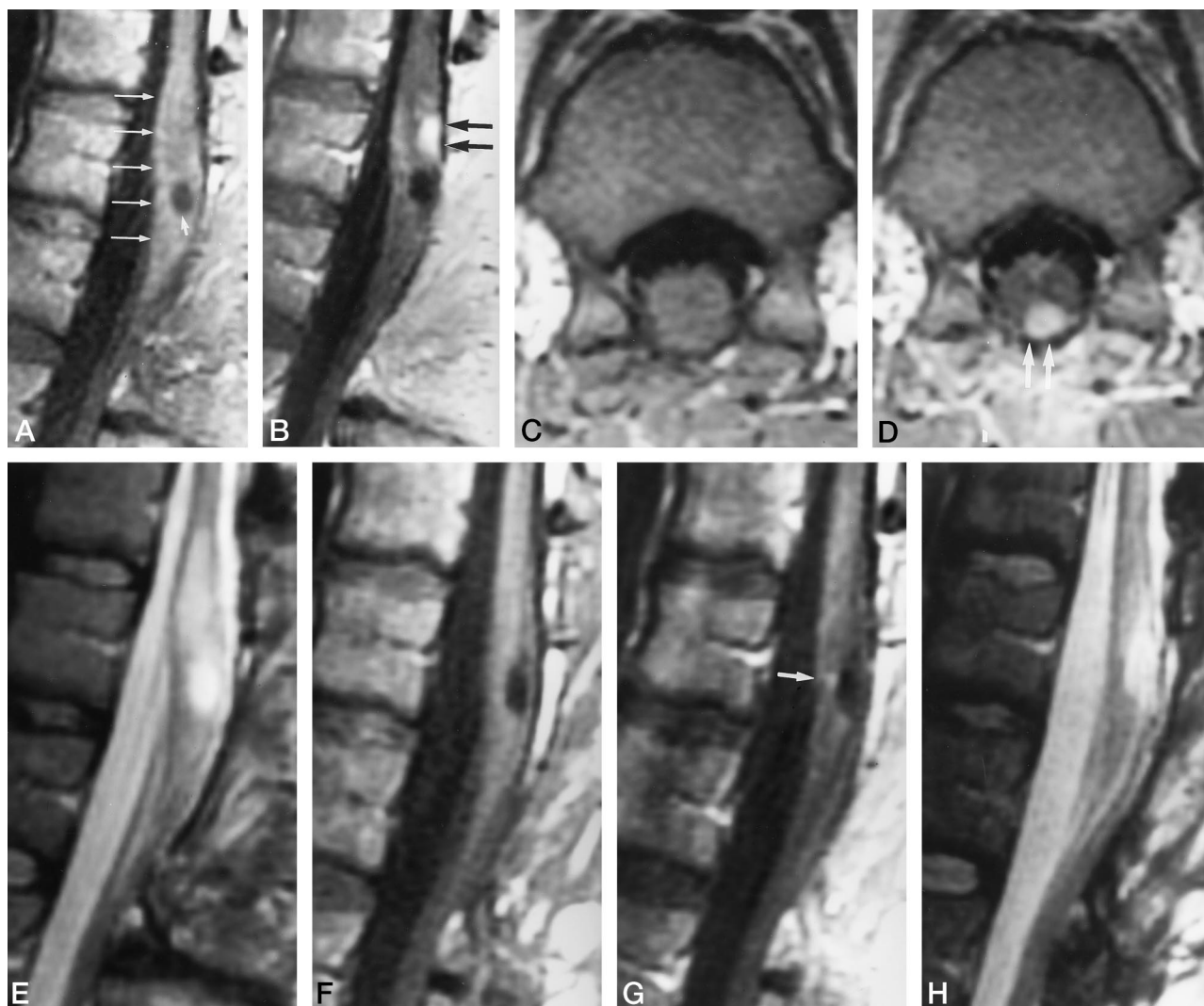
FIG 2.   Case 2: *M fortuitum* intramedullary abscess in a 31-year-old man with a 10-day history of increasing lower back pain with pain and sensory changes in both lower extremities. He underwent laminectomy at T12-L1 at another institution. *M fortuitum* was cultured from the spinal cord tissue obtained during surgery. Decreased sensation in the left lower extremity was noted at the 9-month clinical follow-up.

A–E, T1-weighted sagittal and axial (T-12 level) images before (*A* and *C*) and after (*B* and *D*) contrast administration show widened anteroposterior and transverse dimensions of the distal cord and conus (*long arrows, A*) with intramedullary patchy and solid contrast enhancement (*arrows, B* and *D*) with central hypointensity (*short arrow, A*), which is most prominent posteriorly. T2-weighted image (*E*) shows edema extending from the conus to the T-12 level.

F–H, Four months later, sagittal T1-weighted images without (*F*) and with (*G*) contrast show a persisting cyst and punctate regions of enhancement (*arrow, G*) at the margins of the cyst. On the T2-weighted image (*H*) there is less edema and a decrease in the anteroposterior diameter of the terminal portion of the spinal cord.

ment of systemic lupus erythematosus. None was human immunodeficiency virus (HIV) positive.

Tissue and microbiological (serology and polymerase chain reaction) confirmation of the specific infectious agent was available in four cases (mycobacteria in two cases, *Schistosoma* organisms in one case, and streptococcus in one case). Two patients, one infected by atypical *Mycobacterium fortuitum* and the other by *S mansoni*, underwent a laminectomy and decompression with subtotal resection of the conus. One patient had a bronchoscopic biopsy confirming cerebrospinal fluid cultures of *M tuberculosis*. Another patient had stereotactic brain biopsy of a concomitant ring-enhancing lesion confirming *Streptococcus milleria* as the organism responsible. Blood, cerebrospinal fluid (CSF) culture, and serologic (enzyme-linked immunosorbent assay [ELISA]) test results were available in two cases (one with schistosomiasis and one with streptococcosis).

Results

The organisms responsible for these intramedullary infections were *M tuberculosis* (Fig 1), atypical *M fortuitum* (Fig 2), *S pyogenes* group A (Fig 3), *S milleria* (Fig 4), and, in two cases, *S mansoni* (Fig 5). All caused similar imaging changes in the cord. The initial imaging studies (see Table) showed areas of intramedullary high signal on proton density– and T2-weighted sequences (Fig 4C). The unenhanced T1-weighted sequences showed an increase in cord diameter (Fig 4B). After administration of contrast material, poorly defined marginal enhancement was visible on T1-weighted images (Fig 4E). This abnor-

FIG 3. Case 3: group A streptococcus intramedullary abscess in a 74-year-old man with fever, chills, profound bilateral lower extremity weakness, and incontinence of stool and urine. Blood and CSF cultures (4/4 bottles) yielded *S pyogenes.* Symptoms resolved after 3 months of penicillin treatment.

A, Sagittal contrast-enhanced T1-weighted image shows widening of the anteroposterior diameter of the cord and low signal intensity in the conus. These is minimal enhancement (*arrows*) around the region of low signal intensity.

B, T2-weighted image shows high signal intensity in the central portion of the spinal cord (*arrowheads*).
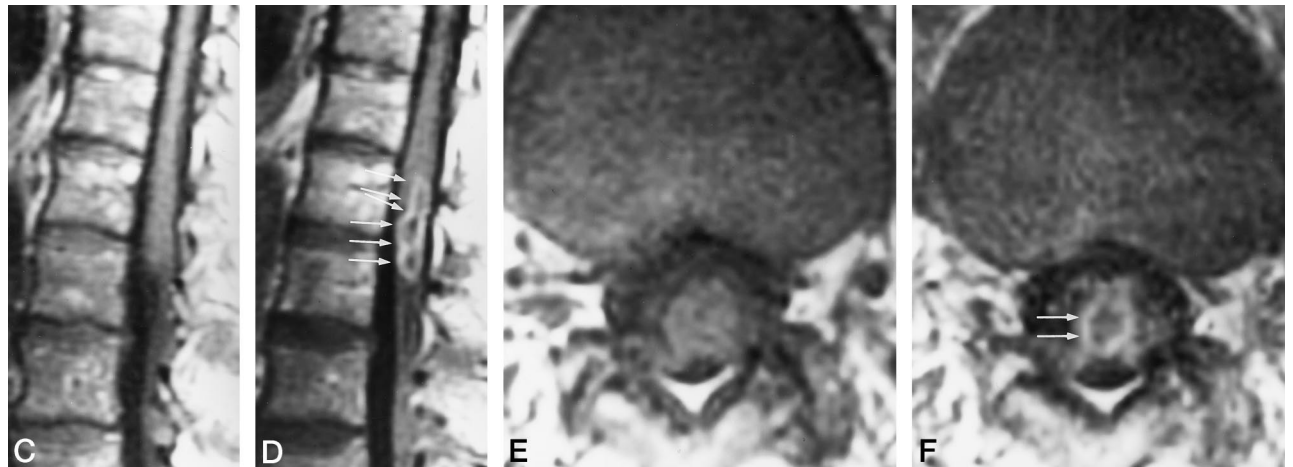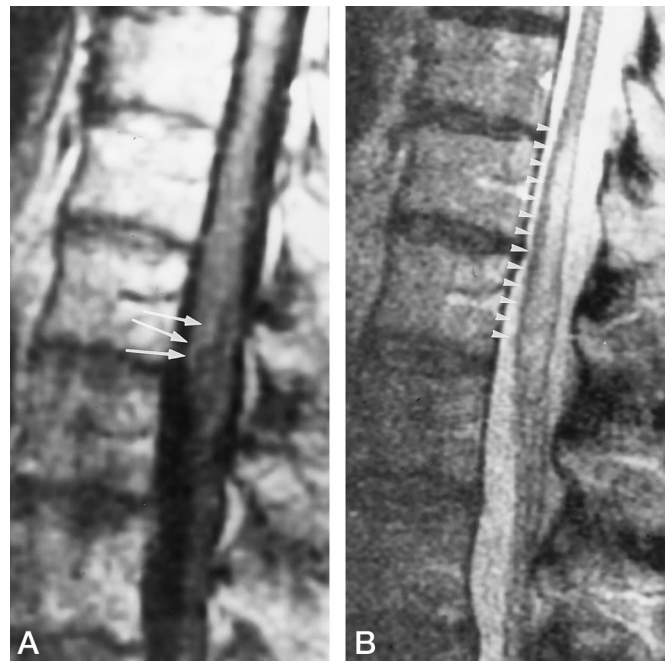
C–F, One week later, T1-weighted sagittal (*C*) and axial (*E*) images at the T-12 level before (*C* and *E*) and after (*D* and *F*) contrast administration show widened anteroposterior and transverse dimensions of the spinal cord with ring enhancement extending to the surface of the spinal cord (*arrows, D* and *F*).

G, T2-weighted image shows intramedullary high signal at and above the conus (*arrowheads*).

H–I, Three months later, sagittal contrast-enhanced T1-weighted image shows subtle abnormal intramedullary enhancement (*arrows, H*) in the conus. The T2-weighted image shows resolution of edema with a central region of low signal intensity, possibly representing hemosiderin deposition (*arrows, I*).
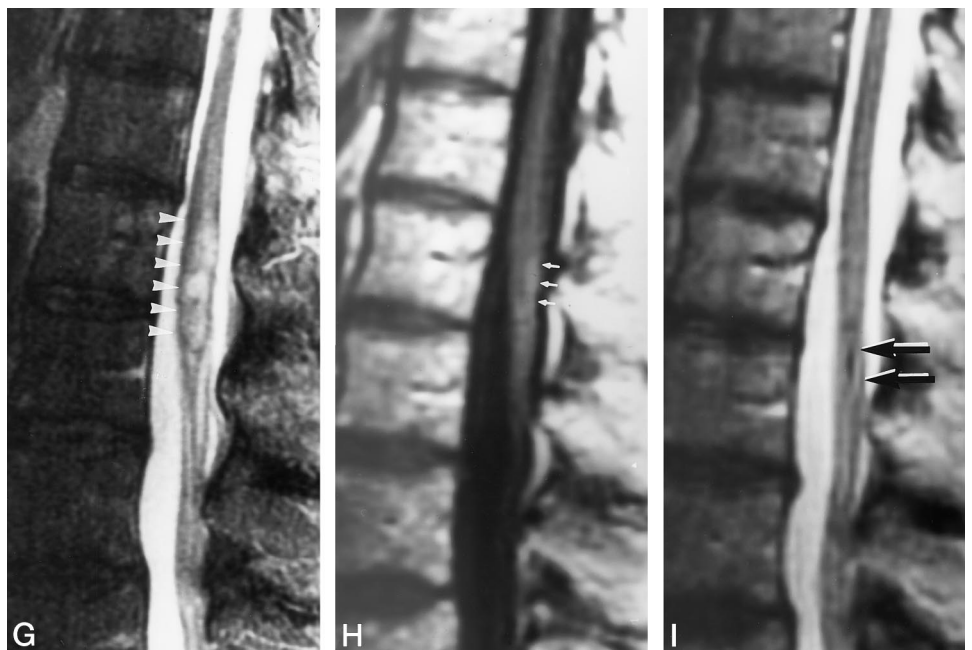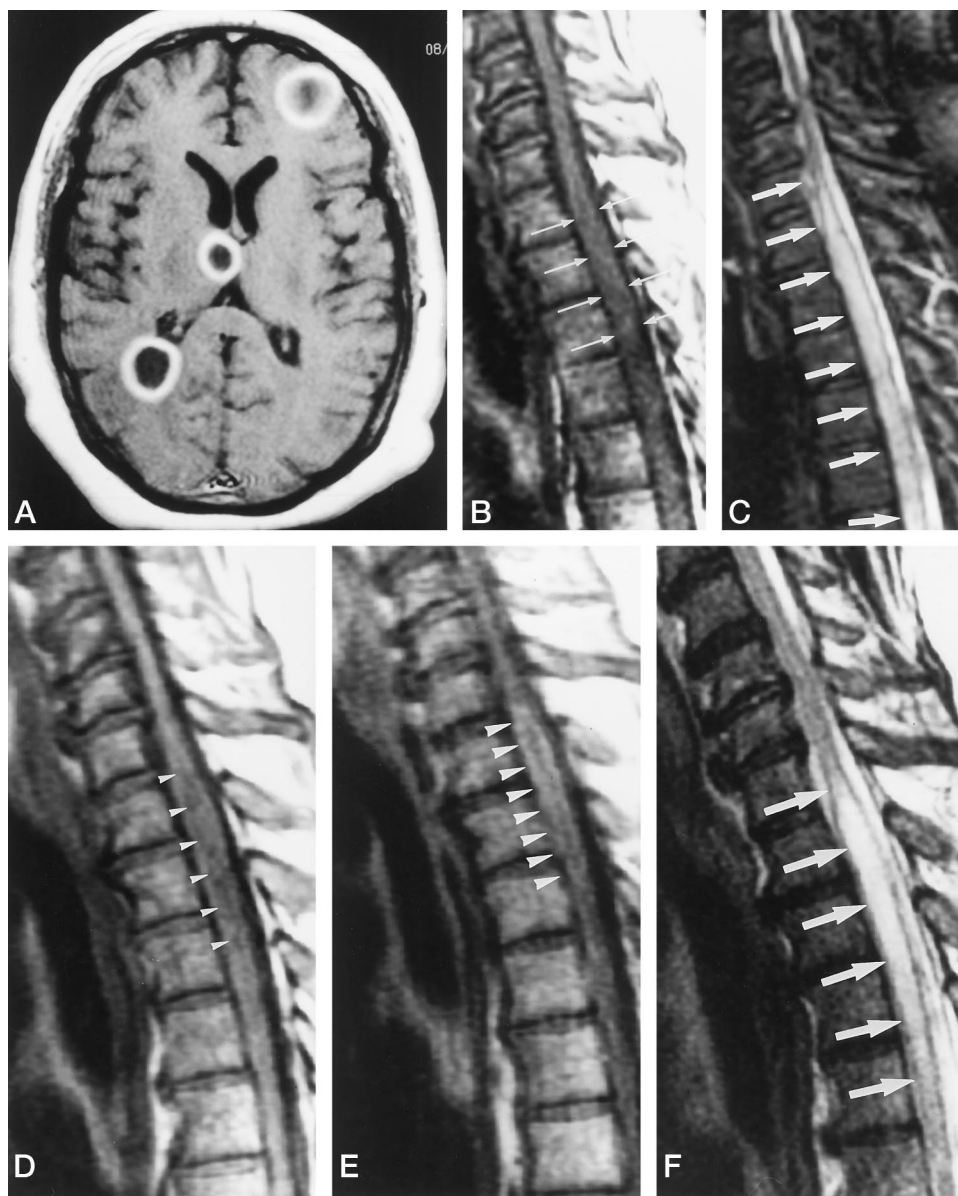
Fig 4. Case 4: *S milleria* intramedullary abscess in 45-year-old man with lower back pain, fever, and lower extremity paralysis. Culture of tissue obtained from a stereotactic biopsy of a ring-enhancing brain lesion revealed infection with *S milleria*. At 2-month clinical follow-up the patient had sensory disturbances in both lower extremities.

A, Brain MR image reveals multiple intracranial ring-enhancing lesions at the gray/white matter junction.

B and *C*, Initial unenhanced T1-weighted images of the spine show an increase in anteroposterior diameter of the spinal cord beginning at the upper thoracic levels (*arrows, B*). Signal intensity is markedly increased on T2-weighted image (*arrows, C*).

D–F, Ten days later, after initiation of antibiotic therapy, there is continued cord swelling with central, decreased signal intensity on T1-weighted image (*arrowheads, D*). After contrast administration there is faint ring enhancement extending to the surface of the spinal cord (*arrowheads, E*). On T2-weighted image, there is less caudal extension of the thoracic cord edema (*arrows, F*).

mal enhancement was more localized than the diffuse and more extensive T2 high signal abnormality, which generally extended for several segments above and below the enhancing lesion (Fig 1G and H). After the initiation of therapy, the T2 signal abnormalities markedly decreased in size and in prominence (Fig 4C and F). Additionally, the regions where subtle, poorly defined marginal enhancement had been seen on pretreatment studies showed well-defined ring-enhancing margins with central low signal on post-contrast T1-weighted images, consistent with abscess formation (Fig 3A and D). These areas of enhancement resolved with treatment, as seen on serial imaging studies (Figs 1G and J, and 2B and G). An anatomic site of preferential involvement in the distal thoracic cord and conus was identified in all patients. Two patients also had multiple intracranial abscesses at the gray/white matter junction (Fig 4A). The brain lesions responded over the same time course as did the cord lesions. None of the patients had MR evi-

dence of arachnoiditis. At clinical follow-up, one patient had normal findings, two had gate disturbance (one mild, one moderate), two had abnormal sensation in the lower extremities (one bilateral, one unilateral), and one had bowel, bladder, and gate disturbance.

Discussion

The symptoms of spinal cord are indistinguishable from those of epidural abscess. Most are of hematogenous origin, and the primary source is usually the respiratory tract (Figs 1–3). Intramedullary abscess may also complicate congenital dermal sinuses or bacterial endocarditis. Because the disease process is so rare, there is relatively little accumulated experience in the management of intramedullary abscess (4). Treatment consists of a several-month course of antibiotic administration for bacterial processes and at least a year of therapy for mycobacterial condi-
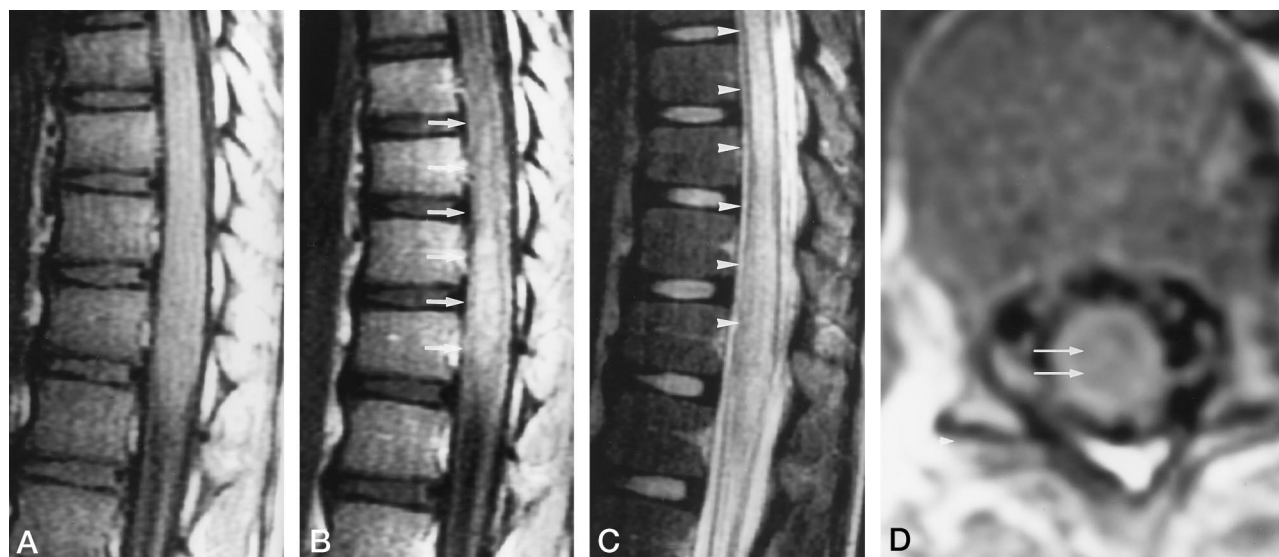
FIG 5. Case 5: *S mansoni* intramedullary abscess in an 11-year-old boy who had recently immigrated to the United States from Yemen. He presented with bilateral lower extremity weakness progressing over 7 days to paraplegia. Diagnosis was based on schistosomiasis antibody from serum and CSF (result, 6.87 IU; normal, <1.0 IU). At 5-month clinical follow-up, the patient had minimal residual lower extremity weakness.

A–E, T1-weighted sagittal and axial (T-12 level) images before (*A* and *D*) and after (*B* and *E*) contrast administration show widened anteroposterior and transverse dimensions of the spinal cord with low central signal intensity (*arrows, D*) and with intramedullary contrast enhancement (*arrows, B* and *E*), most prominent anteriorly. The initial T2-weighted image shows abnormal high signal in the distal cord and conus (*arrowheads, C*).

F–G, Five months later there is no persisting abnormal enhancement after contrast administration (*F*), and signal intensity on T2-weighted image is normal (*G*).

tions. Medical therapy alone may be attempted, but laminectomy and surgical debridement are indicated if neurologic symptoms progress during medical therapy. However, because the illness is uncommon, a consensus on the indications for neurosurgical intervention has not been established (4).

In an attempt to understand the pathogenesis and imaging alterations associated with spinal cord abscesses, it has been suggested that the development of this process may be associated with focal venous infarcts that are complicated by bacterial colonization (9, 10). Sequential imaging findings in our series of patients suggest that the development of abscess within the spinal cord may be similar to the pathologic evolution of abscess in the brain, the serial imaging characteristics and histology of which have been described in detail in animals and humans (11, 12). The serial spinal cord images of our patient group, as well as of a patient with intramedullary

spinal cord infection who was excluded from our study because of disk and epidural space infection, reveal the same imaging progression that has been documented in the brain (11). T2-weighted MR images of brain tissue obtained during the phase of early cerebritis initially show high signal, with poorly defined enhancement on postcontrast T1-weighted images. Identical findings were seen in our patients with cord infections, and we termed this phase the early stage of infectious myelitis (Fig 4B and D). Approximately 1 week after the initiation of treatment, the region of myelitis became less diffusely hyperintense on T2-weighted sequences, with more clearly defined marginal enhancement on postcontrast T1-weighted images (Fig 4F). The surrounding edema continues to be more extensive than the margins of enhancement. We term this phase the late stage of myelitis, and postulate that it corresponds to capsular formation and to the inflammatory and vascular correlates of

Six patients with intramedullary cord abscess

Case	Organism	No. of Studies	Level of Abnormal T2 Signal	Expansion	Findings on Contrast-Enhanced MR Images	Findings at MR Follow-up	Clinical Outcome
1	*M tuberculosis*	4	Distal cord, conus	Yes	Solid enhancement	At 5 wk, solid and ring enhanced	At 7 mo, gait disturbance
2	*M fortuitum*	2	Distal cord, conus	Yes	Solid enhancement, slight central hypointensity	At 4 mo, peripheral enhanced cavity	At 9 mo, decreased sensation in L leg
3	Group A *S pyogenes*	3	Distal cord, conus	Yes	Peripheral, poorly defined enhancement	At 1 wk, ring-enhanced abscess	At 3 mo, resolution of symptoms
4	Group D *S milleria*	3	T-1 to distal cord	No	Peripheral, poorly defined	At 10 d, ring-enhanced abscess	At 2 mo, lower limb sensory disturbance
5	*S mansoni*	2	Distal cord, conus	Yes	Solid with slight central hypointensity "ricelike" areas	At 5 mo, normal	At 5 mo, minimal residual gait disturbance
6	*S mansoni*	1	Distal cord, conus	Yes	Patchy central "ricelike" areas	· · ·	At 3 mo, gait and bowel/bladder disturbance

imaging described as the late stage of cerebritis by Enzmann et al (11). The earliest that well-defined enhancement was seen in our series was on a study 7 days after presentation (Fig 3D and F). This finding is thought to represent the beginning of intramedullary cord abscess formation. The central cavitary portions of the intraaxial necrotic areas are seen on T1-weighted noncontrast images as areas of low signal intensity and as hyperintense foci on T2-weighted sequences. While regions of hyperintense signal on T2-weighted sequences were seen to subside over several weeks, the foci on T1-weighted postcontrast images slowly diminished in size for several months (Fig 1J and K). In all patients, the initial T2-weighted sequences showed more extensive cord abnormality than did the postcontrast T1-weighted studies (Fig 1E and B).

Among the causes of spinal cord abscesses are important epidemiologic, social, and pathogenic differences that may relate to diagnosis, treatment, and outcome. Human schistosomiasis, for example, is not endemic in the United States. Approximately 200 million people are, however, infected with schistosome worms worldwide, and immigration and travel are increasingly bringing these patients to medical attention in this country (13). Adult schistosome worms can live and produce eggs for many years after the host has left the endemic area. Schistosome eggs spread to the central nervous system through intraabdominal vertebral and spinal veins. The smallest variety, *S japonicum,* can travel to the brain. *S mansoni* and *S haematobium,* because they have larger capsular spines than *S japonicum,* tend to be deposited in the spinal cord. *S mansoni* has a smaller spine than *S haematobium* and may infect the thoracic cord, while *S haematobium* tends to infect the conus region. Four manifestations of schistosomiasis occur in the spinal cord: 1) asymptomatic deposition of eggs in the cord, 2) confluent granulomatous intramedullary mass in the distal cord, 3) radicular involvement with granulomatous involvement around the conus and cauda equina, and 4) acute transverse myelitis subsequent to diffuse granulomatous changes. Granuloma-

tous intramedullary masses in the distal cord are responsible for 78% of reported cases (14). Comparison of our cases with those in the literature reveals a characteristic pattern on sagittal T1-weighted postcontrast images of enhancing intramedullary foci, which we liken to grains of rice (Fig 5B). The T2 signal alteration in our series was far more extensive than the region on T1-weighted postcontrast images (Fig 5C).

Diagnosis can be made conclusively via serum antibody tests (ELISA) for schistosomiasis, which are available from the Centers for Disease Control. Praziquantel is the treatment of choice. Short courses of steroids are sometimes also administered. Occasionally, laminectomy and partial resection are necessary to decompress the expanded cord (1, 13). With appropriate treatment, residual neurologic defects are surprisingly infrequent. Relapses, however, are not uncommon, as not all eggs may be killed with the first treatment (2).

Bacterial abscess in the spinal cord has been postulated to occur only in a setting of systemic bacteremia (1). In our group, bacteremia was documented by positive blood cultures in both patients with streptococcal myelitis (Figs 3 and 4). In 25% of the patients, however, a primary source of infection is never found (1). It has also been suggested that patient outcome may relate to the rapidity of onset of symptoms. Patients with symptoms of less than 4 days' duration have a mortality rate of 90%, whereas those with symptoms lasting more than 7 days have a mortality of 67% (5, 7). *Staphylococcus* and *Streptococcus* organisms have been the ones most commonly found in intramedullary abscesses (6).

Tuberculosis is undergoing a national resurgence, particularly among HIV-infected persons but also in the immunocompetent population (15). Tuberculous myelitis is, in most cases, associated with tuberculous intracranial involvement of the meninges or brain parenchyma, or with tuberculous arachnoiditis of the spine (16). The imaging features may include irregular cord surface, clumped nerve roots, arachnoid cysts, and secondary syrinx formation within the cord

(17). Intramedullary tuberculomas (Fig 1B) are uncommon and have imaging characteristics similar to those of their intracranial counterparts (18).

Cerebral infarction is a common complication of central nervous system tuberculosis, arising in part from involvement of arterial vessels as they course through basal meningeal exudate (9). A similar potential mechanism did not appear to be operative in our patient population in that none of the six patients in our series had a history of preexisting cord ischemia or presenting symptoms suggestive of acute cord infarction, and all improved clinically after therapy. Additionally, there was no nerve root or meningeal enhancement to suggest meninges-related vascular inflammation as a cause of arterial or venous cord infarction. It is possible, however, that the cord expansion and edema seen in five of these six patients were associated with compromised cord perfusion and relative ischemia.

The differential diagnostic considerations of an intramedullary abscess includes cord ischemia, Guillain-Barré syndrome, acute disseminated myelitis, multiple sclerosis, hemangioblastoma, or other cavitating cord tumors. Serial imaging combined with microbiological and serologic evaluation of CSF, blood, and tissue can correctly identify protozoal or bacterial abscesses. We suggest that the radiologic management of this group of patients should focus on the clinically involved cord segment. Imaging of the entire spine or brain is not indicated unless the patient's clinical status indicates its necessity.

Conclusion

Infection within the spinal cord initially appears as regional, increased signal intensity on T2-weighted images and as poorly defined enhancement on postcontrast T1-weighted images. In our series, ring enhancement was not seen during the myelitis phase at the time of clinical presentation; however, subsequent imaging, after at least 7 days, revealed ring enhancement and development of true intramedullary cord abscess. An anatomic site of preferential involvement in the distal thoracic cord and conus medullaris was identified in all six patients studied. The diagnosis of septic myelitis needs to be considered in any patient with intramedullary high signal intensity and abnormal contrast enhancement on T2-weighted images.

References

1. Babu R, Jafar JJ, Huang PP, Budzilovich GN, Ransohoff J. **Intramedullary cord abscesses associated with spinal cord ependymoma: case report.** *Neurosurgery* 1992;30:121–124
2. **Case records of the Massachusetts General Hospital: case 4–1996.** *N Engl J Med* 1996;334:382–389
3. Courville CB. *Pathology of the Central Nervous System.* 3rd ed. Mountain View, Calif: Pacific Press; 1950:191–192
4. Ditullio MV. **Intramedullary spinal abscess: case report with a review of 53 previously described cases.** *Surg Neurol* 1977;7:351–353
5. Blacklock TB, Hood TW, Maxwell RE. **Intramedullary cervical cord abscess.** *J Neurosurg* 1982;57:270–273
6. Menezes AH, Van Gilder JC, Perret GE. **Spinal cord abscesses: a review.** *Surg Neurol* 1977;8:461–467
7. Maurice-Williams RS, Pamphilon D, Coakham HB. **Intramedullary spinal cord abscess: a rare complication of spinal dysraphism.** *J Neurol Neurosurg Psychiatry* 1980;43:1045–1048
8. Hart J. **Case of encysted abscess in the center of the spinal cord.** *Dublin Hosp Rep* 1830;5:522–524
9. Sharif HS. **Role of MR imaging in the management of spinal infections.** *AJR Am J Roentgenol* 1992;155:1333–1345
10. Keener BS, Daras M, Duffy KR. **Abscess formation in the spinal cord.** *Brain* 1955;78:394–400
11. Enzmann D, Britt R, Yeager A. **Experimental brain abscess evolution: computed tomographic and neuropathology correlation.** *Radiology* 1979;133:113–122
12. Haimes AB, Zimmermann RD, Morgello S, et al. **MR imaging of brain abscesses.** *AJNR Am J Neuroradiol* 1989;10:279–292
13. Silbergleit R, Silbergleit R. **Schistosomal granuloma of the spinal cord: evaluation with MR imaging and intraoperative sonography.** *AJR Am J Roentgenol* 1992;158:1351–1353
14. Scrimgeor EM, Gajdusek DC. **Involvement of the CNS in schistosomiasis mansoni: a review.** *Brain* 1985;108:1023–1038
15. Whiteman M, Espinoza L, Donovan Post MJ, Bell MD, Falcone S. **Central nervous system tuberculosis in HIV-infected patients: clinical and radiological findings.** *AJNR Am J Neuroradiol* 1995;16: 1319–1327
16. Chang KH, Han MH, Kim IO, Har MH, Kim CW. **Tuberculous arachnoiditis of the spine: findings in myelography, CT, and MR imaging.** *AJNR Am J Neuroradiol* 1989;10;1255–1262
17. Kumar A, Montanera W, Willinsky R, TerBrugge KG, Agarwal S. **MR features of tuberculous arachnoiditis.** *J Comput Assist Tomogr* 1993;17:127–130
18. Jena A, Banerji AK, Tripathi RP, et al. **Demonstration of intramedullary tuberculomas by magnetic resonance imaging: a report of two cases.** *Br J Radiol* 1991;64:555–557